

My Approach to Functional Analysis in Computed Tomography Angiography: Myocardial Perfusion and FFRct

Gustavo Corrêa de Almeida Teixeira,¹ Bruno Vicente Gomes de Castro,^{1,2} Douglas Carli Silva,^{3,4} Tiago Magalhães^{1,5}

Teleimagem, Imagem Cardiovascular,¹ São Paulo, SP – Brazil

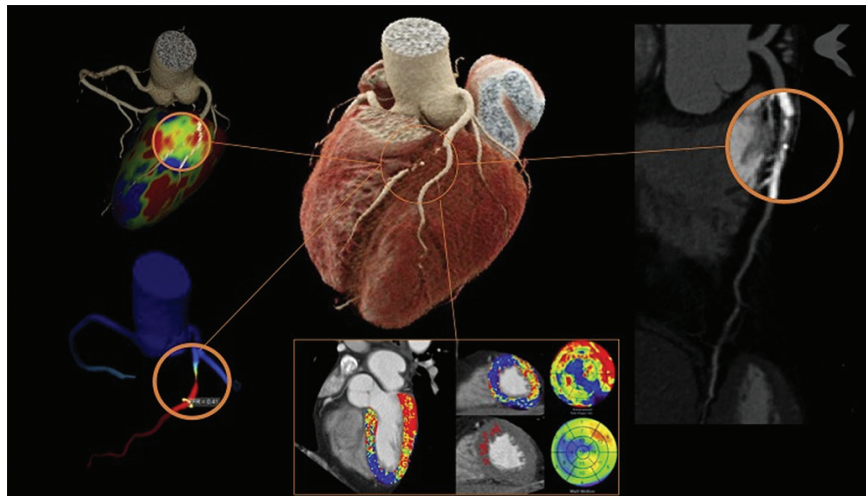
CEDIP Medicina Diagnóstica,² Curitiba, PR – Brazil

Siemens Healthineers AG,³ Erlangen, Bayern – Germany

Instituto de Radiologia do Hospital das Clínicas FMUSP,⁴ São Paulo, SP – Brazil

Hospital do Coração, Diagnóstico por Imagem,⁵ São Paulo, SP – Brazil

Central Illustration: My Approach to Functional Analysis in Computed Tomography Angiography: Myocardial Perfusion and FFRct



Arq Bras Cardiol: Imagem cardiovasc. 2024;37(4):e20240113

Coronary computed tomography angiography (CCTA) combining anatomy and functional assessment in the investigation of coronary disease. **Central panel:** three-dimensional reconstruction of the heart and coronary arteries. **Upper left panel:** 3D coronary tree with perfusion map of the left ventricle demonstrating the region irrigated by the affected artery. **Lower left panel:** fractional flow reserve derived from CCTA (FFRct) with a value <0.80 , compatible with flow-limiting stenosis. **Lower panel:** color-coded myocardial perfusion, demonstrating a perfusion defect under stress related to the region of the left anterior descending artery. **Right panel:** visual anatomical analysis by CCTA, demonstrating a sub-occlusive lesion in the left anterior descending artery.

Abstract

Coronary computed tomography angiography (CCTA) is an effective noninvasive method for detecting atherosclerotic disease, especially in symptomatic patients with low-to-moderate disease probability. Despite good accuracy in detecting obstructions, its

relationship with functional lesion severity is limited. For a more accurate assessment, anatomical evaluation can be associated with myocardial computed tomography perfusion and fractional flow reserve derived from CCTA (FFRct). Myocardial perfusion computed tomography identifies areas of ischemia. FFRct, which assesses the hemodynamic significance of stenoses, has shown high accuracy and can reduce the need for invasive catheterizations. The image acquisition and interpretation protocols are essential to ensure reliable results and appropriate management of patients with coronary artery disease.

Keywords

Computed Tomography Angiography; Myocardial Perfusion Imaging; Myocardial Fractional Flow Reserve

Mailing Address: Gustavo Corrêa de Almeida Teixeira • Teleimagem, Imagem Cardiovascular. Rua Desembargador Eliseu Guilherme, 53, 7º andar. Postal Code: 04004-030, Paraíso, São Paulo, SP – Brazil
E-mail: gustavo.cateixeira@gmail.com
Manuscript received October 31, 2024; revised November 1, 2024; accepted November 1, 2024
Editor responsible for the review: Marcelo Tavares

DOI: <https://doi.org/10.36660/abcimg.20240113>

Introduction

Coronary computed tomography angiography (CCTA), a well-established noninvasive diagnostic method for detecting coronary atherosclerotic disease, has a high negative predictive value and is indicated in symptomatic patients with a low-to-intermediate pre-test probability of obstructive disease. Despite having good

accuracy for detecting obstructive disease, the relationship between detected lesions and their functional severity is low.¹ In recent years, tomographic anatomical analysis has been complemented with ischemia assessment by myocardial computed tomography perfusion and fractional flow reserve derived from coronary computed tomography (CT) (FFRct). These assessments provide additional information, allowing more precise assessment of the repercussions of the identified stenoses.

Combined assessment, such as associating CCTA with myocardial computed tomography perfusion, results in greater specificity and accuracy than CCTA alone. Combining both techniques has better diagnostic performance regarding restenosis of coronary stents and segments whose anatomical assessment is limited due to motion artifacts or excessive calcification. Similar results were found for prognostication of major cardiovascular events within 2 years, being comparable to the combined use of invasive coronary angiography and myocardial scintigraphy.^{2,3}

In turn, tomographic analysis complemented with ischemia assessment by FFRct provides crucial information on patients with coronary artery disease, since ischemia-guided revascularization of lesions (FFR \leq 0.80) detected by invasive FFR measurement reduces the incidence of major adverse cardiovascular events, especially urgent revascularization.⁴

Myocardial computed tomography perfusion

Myocardial computed tomography perfusion assessment uses iodinated contrast before and after administration of vasodilator drugs to identify ischemic areas.⁶ Two main techniques have been described for this assessment. The

“dynamic” technique, which involves serial acquisition of the first contrast passage through the myocardium, and the “static” technique, which is based on a single acquisition during the peak of the initial contrast injection (Figure 1).^{5,6} The dynamic technique can quantitatively evaluate flow, although it requires specific post-processing software. It also requires CT scanners that can cover the entire heart, or at least 2 acquisitions from devices with less coverage which are subsequently merged using the image reconstruction function.⁷

The static perfusion technique, however, has a simpler and more accessible acquisition protocol on machines with less coverage and allows visual interpretation of the images (qualitative), eliminating the need for post-processing software.⁸ Due to its greater clinical applicability (it can be performed by CT scanners with \geq 64 detector columns), this article will describe the static perfusion protocol.

Two acquisitions are necessary for the perfusion assessment, one at rest, which is also used to assess coronary anatomy, and another after the use of a coronary vasodilator drug, with an interval of 10 to 15 minutes between acquisitions.⁹

Although the order of acquisitions (stress/rest or rest/stress) does not appear to affect the results, the techniques have certain advantages and disadvantages. Some authors report that performing the stress sequence first avoids artifacts secondary to residual contrast, which can be confused with perfusion defects. However, beginning with the rest sequence would prioritize coronary luminal evaluation and, if potentially obstructive coronary lesions are not visualized, the stress sequence may not be necessary.¹⁰

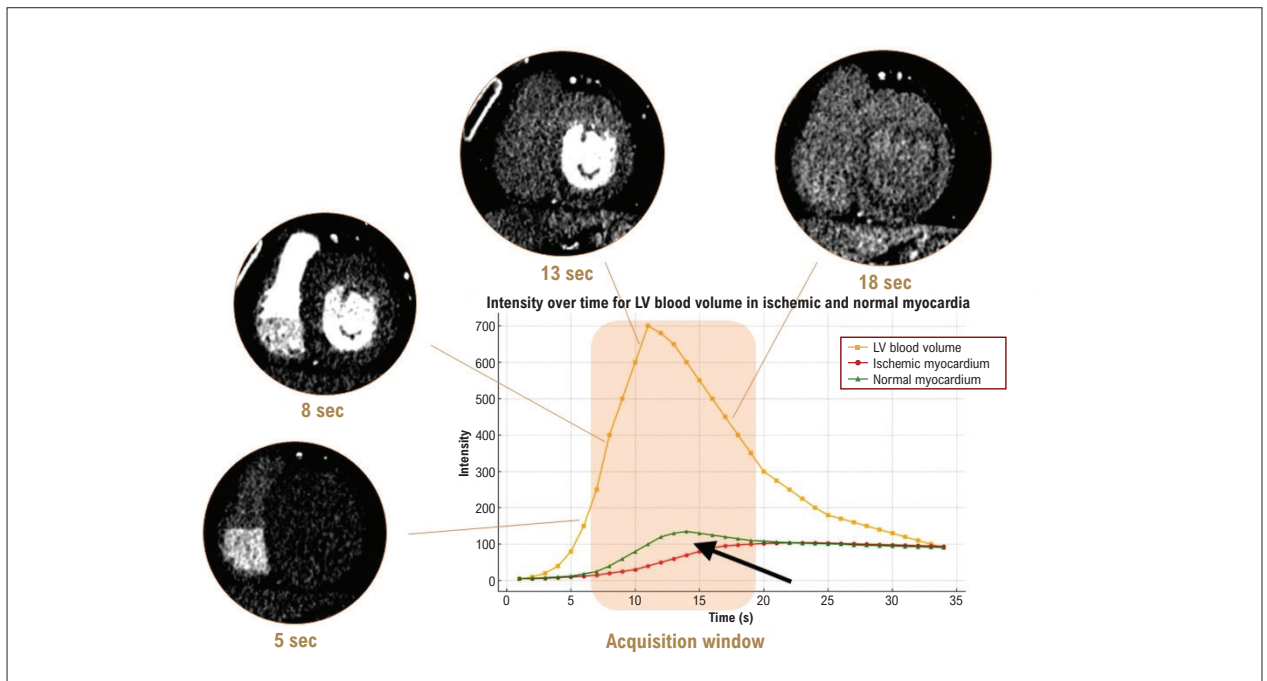


Figure 1 – Intensity of the myocardial and ventricular cavity attenuation curves over time. Relative hypoattenuation of the ischemic myocardium occurs close to the peak of ventricular cavity contrast enhancement. The difference in attenuation between a normal and ischemic myocardium (arrow) represents myocardial ischemia, which is identified in the first injection of iodinated contrast during pharmacological stress (ie, the “acquisition window” for identifying myocardial ischemia). LV: left ventricle.

Acquisition protocol

Adequate preparation is required to effectively obtain the images, including caffeine abstinence in the 24 hours prior to the test. Patients should be assessed for contraindication to dipyridamole, beta-blockers, and nitrates. Heart rate, blood pressure, and electrocardiogram monitoring are also recommended throughout the examination.⁶

Image acquisition at rest should follow the usual CCTA protocols, prioritizing anatomical assessment. However, the stress protocol can be performed at a lower radiation dose.¹⁰

The available stressor agents are dipyridamole, adenosine, and regadenoson, the first of which is the most widely used in our setting and, thus, is suggested. Nitrate and beta-blockers are used to achieve rest following the usual CCTA protocol.⁹ It is important to note that if the rest/stress protocol is selected, a 20-minute interval is required between the application of nitrate and acquisition of stress images.¹⁰

Table 1 presents a suggested protocol for 64-channel CT scanners, including acquisition parameters. Figure 2 presents a flowchart summarizing the acquisition steps.

Image reconstruction and artifact recognition

Some strategies can be suggested to ensure good image reconstruction. One is to reconstruct several phases at each 5% of the R-R interval, allowing identification of the best temporal resolution. It is also essential to reconstruct the images in 3 classic projections: the short, long horizontal, and long vertical axes. These projections allow evaluation of the myocardial regions in 2 distinct axes. Finally, the images should be evaluated in slices of 3-5 mm, and correction filters should be used, if available.⁹

Image interpretation

Image interpretation should follow a systematic approach. The first step consists of evaluating the CCTA, describing and grading the identified stenoses. Uninterpretable segments should also be

described, ie, those whose luminal evaluation was inaccessible due to artifacts, stents, or calcifications. It is important to check for points of myocardial thinning, adipose metaplasia, calcification, ventricular aneurysms or pseudoaneurysms, and mural thrombi, which may indicate or be related to areas of hypoperfusion.¹¹

The images are then evaluated for the presence of hypoattenuation during rest and stress. Hypoattenuation during stress that is reversible at rest suggests myocardial ischemia (Figure 3), while areas of hypoperfusion at rest indicate infarction (fibrosis). It is worth noting that areas of hypoattenuation at rest may show partial improvement, normalization, or even hyperattenuation during stress, a phenomenon known as late hyperattenuation of myocardial scar areas. Finally, areas of hypoattenuation that increase in size during stress suggest peri-infarction ischemia (Figure 4).¹¹ All identified changes must be confirmed in at least two different projections and evaluated in several phases, since true hypoperfusions persist throughout these phases, which is essential to exclude the possibility of artifactual findings.

Finally, a detailed correlation is performed between the areas of hypoperfusion, whether fixed or reversible, and the corresponding coronary artery obstructions. Segments in which the CCTA assessment presented uncertainties, such as moderate lesions, stents, or calcified plaques, can be reclassified according to the identified perfusion defects. Diagnostic uncertainty in association with a perfusion defect strongly suggests the presence of significant stenosis.¹⁰ Combined assessment allows precise identification of the vessels responsible for irrigating a hypoattenuated region, which is useful given the frequent anatomical variation in the coronary tree. In addition, the plausibility of a specific stenosis being responsible for a perfusion defect can be assessed. For example, a perfusion defect in the inferoapical region may be attributed to a long anterior descending artery that bypasses the ventricular apex, demonstrating a correlation between anatomy and function.¹¹ Figure 5 summarizes the steps for image interpretation.

Table 1 – Suggested Myocardial Computed Tomography Perfusion Protocol

Suggested Myocardial Computed Tomography Perfusion Protocol
Pre-exam: abstain from caffeine for 24 hours.
Check contraindications to the use of dipyridamole, beta-blockers, nitrate, and iodinated contrast.
Make 2 access points (18-20 gauge catheters – antecubital veins)
Administer dipyridamole 0.56 mg/kg/4 min (check symptoms, vital signs, and ECG during injection).
Wait 2 minutes after completed injection.
Stress acquisition: retrospective gating; contrast (370 mg/mL) 60 mL at 3 mL/s. Begin acquisition at the peak of left atrial contrast.
Parameters: 100 mA current and 100 Kv tube voltage.
Reverse dipyridamole with aminophylline 240 mg.
Wait 10-15 min between acquisition under stress and acquisition at rest.
Heart rate control (IV metoprolol ≤ 20 mg) until the heart rate is < 65 bpm.
Administer sublingual nitrate 3 min before acquisition at rest.
Acquisition at rest: retrospective gating; contrast (370 mg/mL) 80-90 mL at 5 mL/s.
Parameters: tube current ≤ 850 mA and tube voltage 100 Kv (preferred).

References (2,9). bpm: beats per minute; ECG: electrocardiogram; IV: intravenous; HR: heart rate.

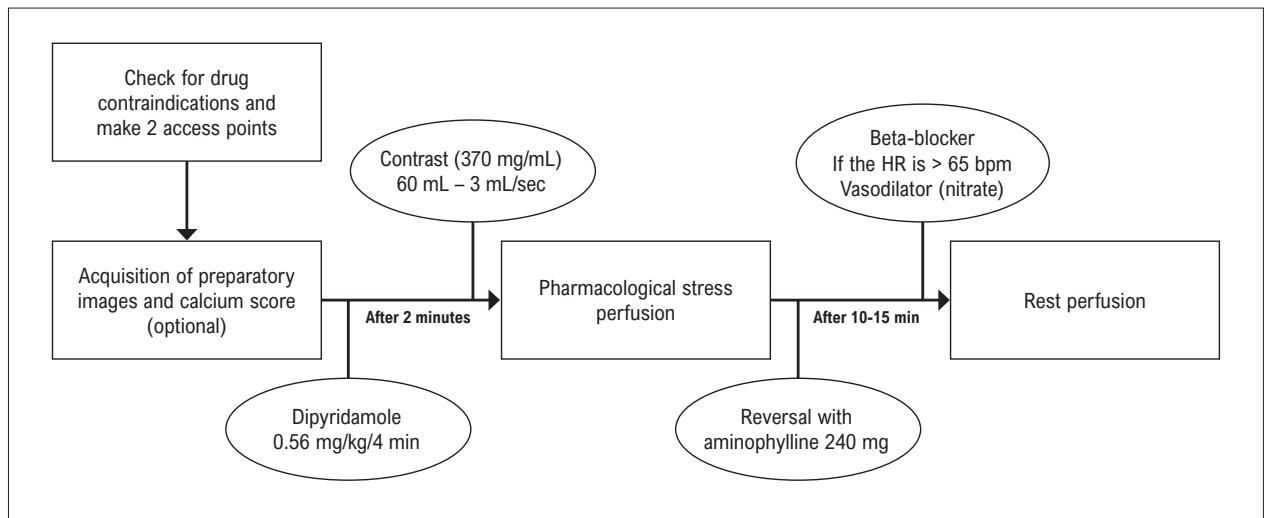


Figure 2 – Acquisition steps of the combined CCTA and myocardial computed tomography perfusion protocol (modified from Magalhães et al.).² bpm: beats per minute; HR: heart rate.

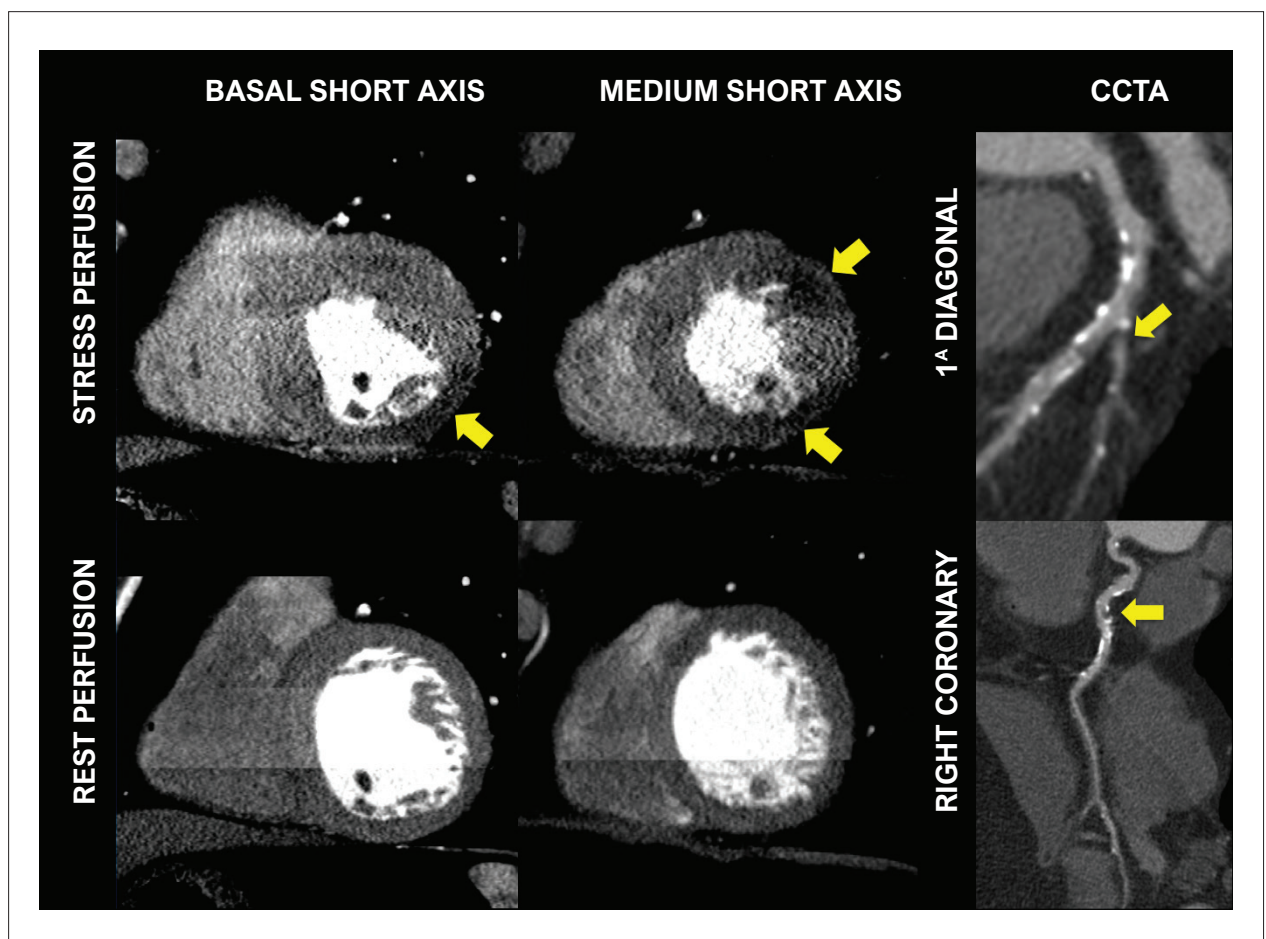


Figure 3 – These images demonstrate a practical case involving combined assessment with CCTA and myocardial computed tomography perfusion. **First stage (anatomical evaluation):** CCTA images demonstrate moderate (questionable) stenosis in the proximal third of the right coronary artery (RCA) and limited evaluation of the ostium of the diagonal branch. **Second stage (perfusion evaluation):** myocardial computed tomography perfusion images reveal reversible perfusion defects in the anterolateral and inferolateral segments, in line with the previously described stenoses. **Third stage (lesion reclassification):** reclassification of the stenoses is plausible. **Fourth stage (anatomical-functional correlation):** the findings indicate flow-limiting stenoses in the diagonal and right coronary branches. CCTA: coronary computed tomography angiography.



Figure 4 – Example of peri-infarction ischemia in the region irrigated by the second marginal branch (Mg2) (hypoattenuation at rest in the inferolateral segment, with an increase in the affected area during stress). There is also ischemia in the region irrigated by the RCA (inferior wall – occluded), which may indicate insufficient collateral circulation. The CCTA images confirm the anatomical plausibility of the perfusion findings.

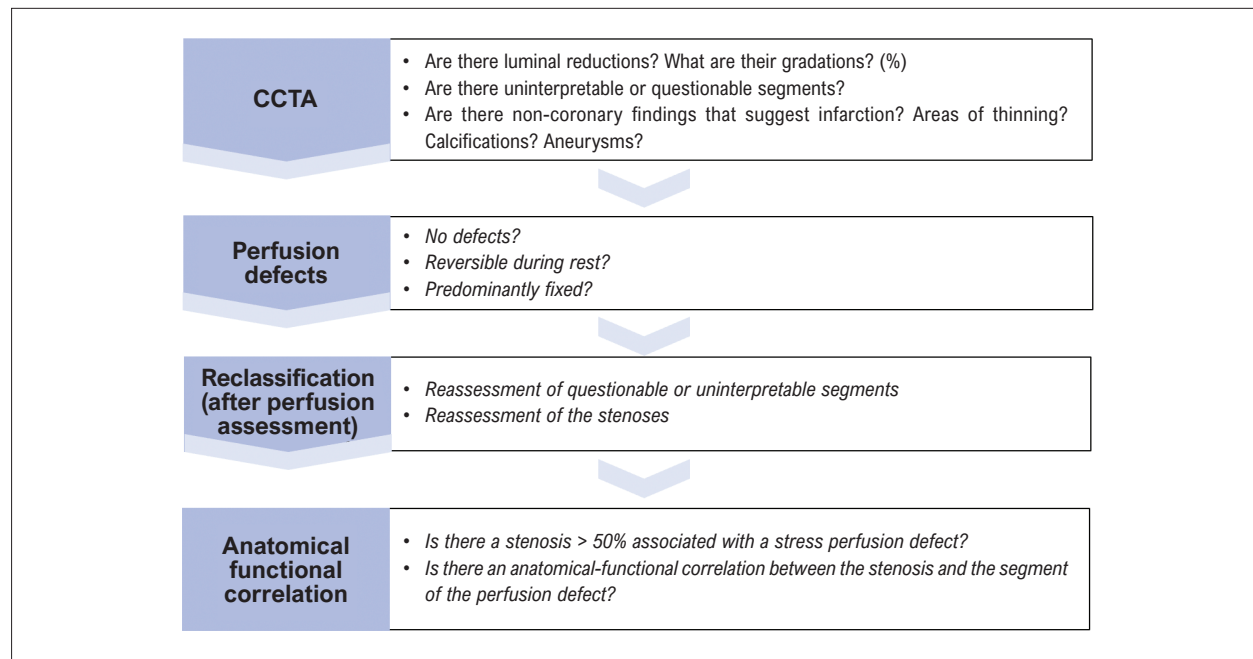


Figure 5 – Combined interpretation of CCTA and myocardial perfusion (modified from Magalhães et al).² CCTA: Coronary computed tomography angiography.

Flow reserve derived from CCTA

The hemodynamic significance of coronary stenoses was initially demonstrated by invasive measurement of fractional flow reserve (FFR) through catheterization, which is considered the gold standard. For FFRct assessment, a 3D

anatomical model of the aortic root and coronary arteries was created, followed by a physiological model derived from the following principles: 1) resting coronary flow is proportional to ventricular mass; 2) microvascular resistance is inversely proportional to vessel size; and 3) reduced microvascular

resistance simulates maximal hyperemia. Finally, dedicated computational algorithms calculate the hemodynamic effects of the stenoses on epicardial circulation.¹² Thus, FFRct can be calculated at each point of the coronary tree from data obtained through a standard coronary tomography, without the need for adenosine or increased patient exposure to ionizing radiation.

The DISCOVER-FLOW study found that FFRct had a diagnostic accuracy of 84.3% and significantly greater specificity than visual analysis by CCTA (82.9% vs 39.6%, respectively).¹³ The DeFacto study did not meet its primary objective of exceeding the lower limit of the confidence interval, but it found better discrimination than CCTA (area under the receiver operating characteristic curve: 0.81 vs 0.68).¹⁴ According to post-hoc analysis, the lack of standardization of beta-blocker and nitrate use may have contributed to the lower diagnostic performance.¹⁵ With an updated software version and more rigorous acquisition protocols, the NXT study found an 81% diagnostic accuracy, 86% sensitivity, 79% specificity, 65% positive and 93% negative predictive values for FFRct in per-patient analysis.¹⁶

In the PLATFORM study, using FFRct as an initial strategy avoided 61% of catheterizations and significantly reduced catheterizations in stenoses $\geq 50\%$ (12% in the FFRct group vs 73% in the invasive group).¹⁷ The multicenter ADVANCE study found great prognostic value for FFRct, with revascularization rates of 38.4% and 5.8% in those with FFRct ≤ 0.80 and FFRct > 0.80 , respectively.¹⁸

In recent years, new approaches based on machine learning algorithms have been developed to calculate FFRct more quickly. These algorithms use geometric relationships learned from large datasets to predict FFRct values based on anatomical features derived from CCTA, eliminating the need

for complex simulations. The main advantage of this method is the possibility of calculating FFRct directly at the examination site using conventional workstations.¹⁹ Studies with small numbers of patients have demonstrated good accuracy and high reproducibility compared to conventional CCTA in relation to invasive FFR measurement, with a shortened average analysis time.²⁰

Acquisition and interpretation

The examination should be performed using machines with at least 64 detector columns under strict heart rate control with oral and intravenous beta-blockers (including ivabradine when necessary), aiming for a heart rate < 60 bpm, which is associated with sublingual nitrate for vasodilation and better coronary visualization. Finally, apnea training is essential to minimize motion artifacts, which degrade the images.²¹

After image acquisition, post-processing generates an interactive 3D anatomical model, with FFRct values represented by colors ranging from blue to red, and respective values from 1 to 0 at each point of the coronary tree. The colors of normal values (> 0.8) range from blue to green, while abnormal values (< 0.8) range from yellow to orange to red (Figure 6).

Using the lowest FFRct value distal to the stenotic lesion has high sensitivity but low specificity, since there is a gradual decline in FFR in distal coronary segments, even in disease-free individuals. Decreased coronary flow reserve can also be observed in patients who have diffuse atherosclerosis without significant lesions (Figure 7). For these reasons, FFRct should be measured 1 to 2 cm after the stenotic lesion, where it has the best diagnostic performance for detecting ischemia (Figure 8).

Errors in lumen segmentation and misalignment of the centerline can generate an inaccurate 3D model, reducing the

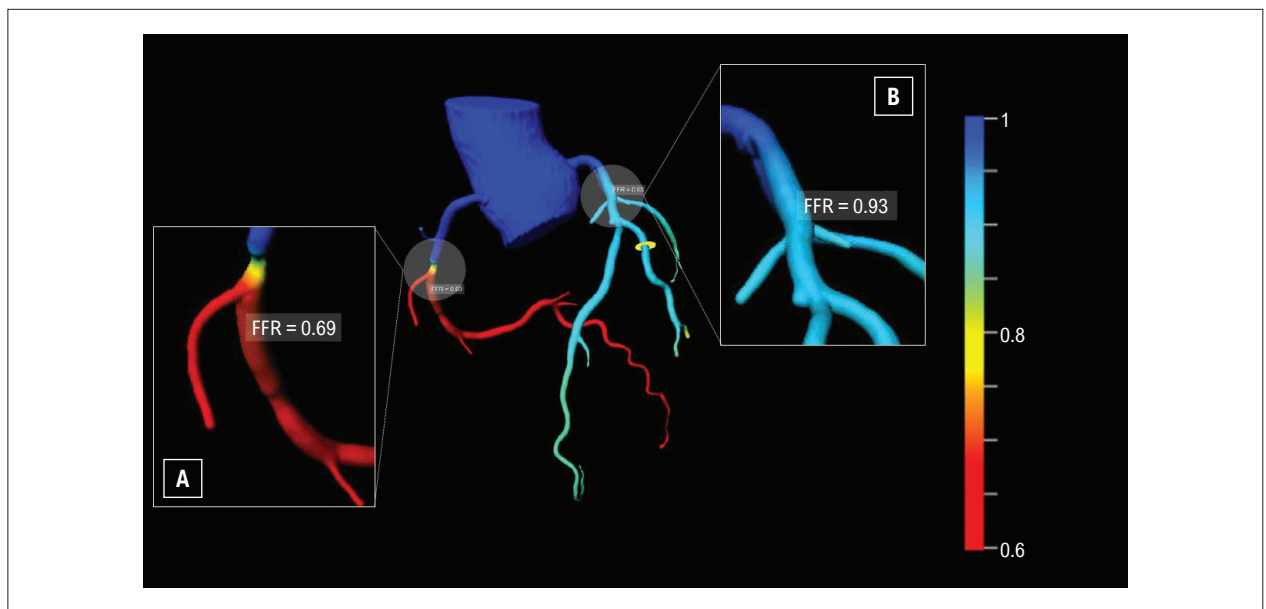


Figure 6 – Three-dimensional model of FFRct in the coronary tree. FFRct values > 0.80 in blue and green, and values < 0.80 in yellow, orange, and red. (A) Lesion in the middle third of the RCA, with abnormal values, suggesting flow-limiting stenosis, (B) Proximal third of the left anterior descending artery with normal FFRct values (> 0.8), without obstructions of hemodynamic significance. FFR: fractional flow reserve.

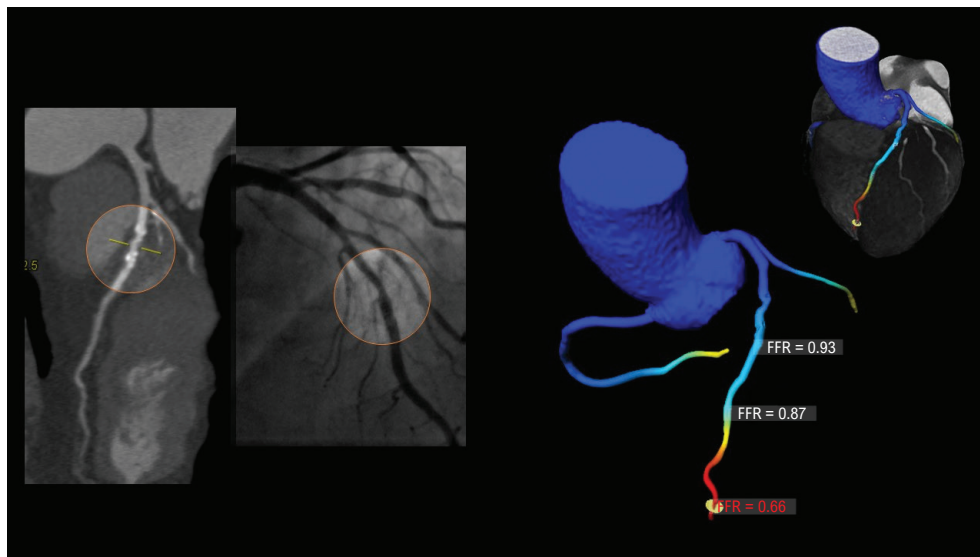


Figure 7 – Male patient, 82 years old, with atherosclerosis in the middle third of the left anterior descending artery, without causing significant luminal reductions. A gradual decrease in pressure was observed along the vessel, with a FFRct value of 0.66 at its nadir. However, following the recommendations for FFRct analysis (1 to 2 cm from the stenotic lesion), the values were within the normal range (>0.8). FFR: fractional flow reserve.

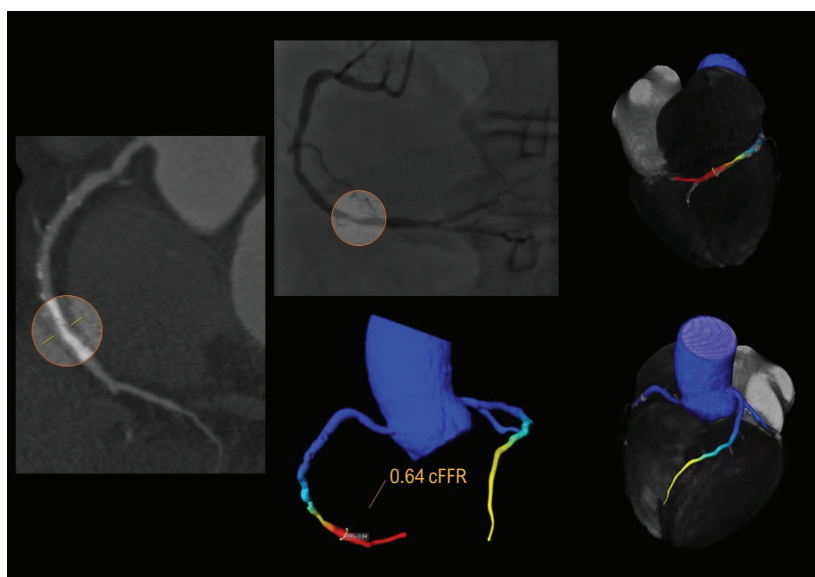


Figure 8 – Male patient, 70 years old, presenting dyspnea on light and moderate exertion. CCTA demonstrating moderate lesion 60 to 70%, and moderate reduction in catheterization. FFRct was performed at 2 cm from the lesion, with a value of 0.64, compatible with flow-limiting stenosis.

method's accuracy.¹² Although calcification impedes stenosis interpretation in CCTA, there were no significant differences in the diagnostic performance of FFRct, even in patients with calcium scores > 400.^{15,22}

Research on FFRct is limited, especially in clinical scenarios such as microvascular disease and the presence of stents and coronary grafts.

Figures 9 and 10 show additional clinical cases illustrating the added value of functional assessment by FFRct in patients with coronary stenoses identified by CTA.

Acknowledgements

The authors would like to thank Siemens Healthineers for providing images and support.

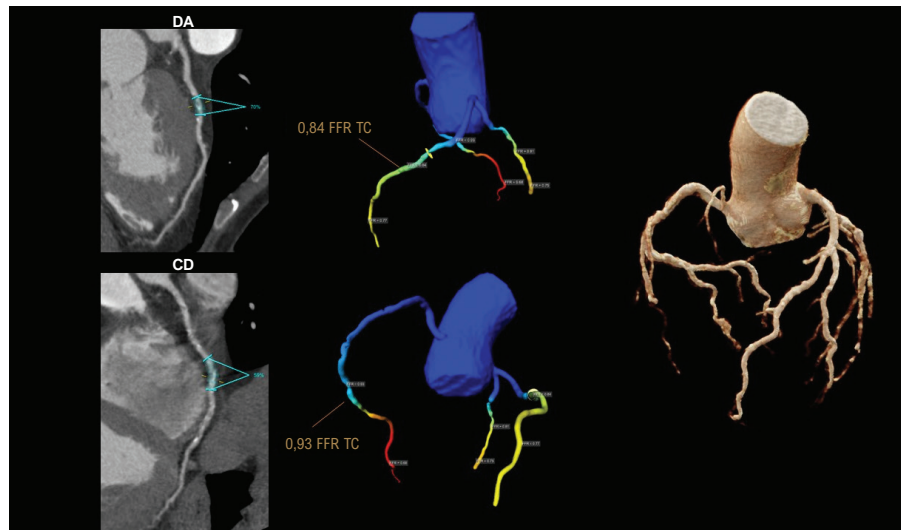


Figure 9 – Case 1: A 67-year-old male patient presented with atypical angina on moderate exertion. CTA demonstrated diffuse atherosclerotic disease with an elevated calcium score of 434. (A) Middle third of the left anterior descending artery (LAD) with mixed component plaque, with 70% luminal reduction, and FFRct of 0.84. Middle third of the RCA with mixed component plaque and moderate luminal reduction, with FFRct of 0.93 (Figure 8). The patient was exempted from invasive evaluation, opting for optimized drug therapy.

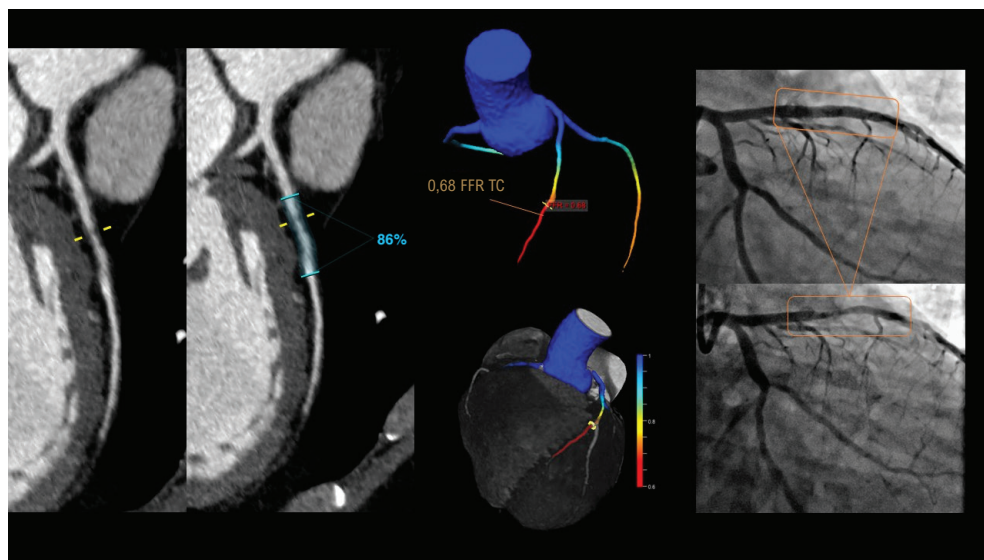


Figure 10 – Case 2: 46-year-old male patient undergoing evaluation for angina. (A) Predominantly non-calcified plaque in the proximal third of the LAD, with significant luminal reduction. (B) FFRct with a value of 0.68, confirming the presence of flow-limiting stenosis. (C) Cardiac catheterization confirming significant luminal reduction (below), with angioplasty with stent performed (above).

Author Contributions

Conception and design of the research and critical revision of the manuscript for intellectual content: Magalhães T; acquisition of data and writing of the manuscript: Teixeira GCA, Castro BVG, Silva DC.

Potential Conflict of Interest

Author declare potential conflict of interest: Douglas Carli Silva – Clinical Specialist at Siemens Healthineers.

Sources of Funding

There were no external funding sources for this study.

Study Association

This study is not associated with any thesis or dissertation work.

Ethics Approval and Consent to Participate

This article does not contain any studies with human participants or animals performed by any of the authors.

References

1. Budoff MJ, Dowe D, Jollis JG, Gitter M, Sutherland J, Halamert E, et al. Diagnostic Performance of 64-Multidetector Row Coronary Computed Tomographic Angiography for Evaluation of Coronary Artery Stenosis in Individuals without Known Coronary Artery Disease: Results from the Prospective Multicenter ACCURACY (Assessment by Coronary Computed Tomographic Angiography of Individuals Undergoing Invasive Coronary Angiography) trial. *J Am Coll Cardiol*. 2008;52(21):1724-32. doi: 10.1016/j.jacc.2008.07.031.
2. Magalhães TA, Kishi S, George RT, Arbab-Zadeh A, Vavere AL, Cox C, et al. Combined Coronary Angiography and Myocardial Perfusion by Computed Tomography in the Identification of Flow-limiting stenosis - The CORE320 Study: An Integrated Analysis of CT Coronary Angiography and Myocardial Perfusion. *J Cardiovasc Comput Tomogr*. 2015;9(5):438-45. doi: 10.1016/j.jcct.2015.03.004.
3. Chen MY, Rochitte CE, Arbab-Zadeh A, Dewey M, George RT, Miller JM, et al. Prognostic Value of Combined CT Angiography and Myocardial Perfusion Imaging versus Invasive Coronary Angiography and Nuclear Stress Perfusion Imaging in the Prediction of Major Adverse Cardiovascular Events: The CORE320 Multicenter Study. *Radiology*. 2017;284(1):55-65. doi: 10.1148/radiol.2017161565.
4. De Bruyne B, Pijls NH, Kalesan B, Barbato E, Tonino PA, Piroth Z, et al. Fractional Flow Reserve-guided PCI versus Medical Therapy in Stable Coronary Disease. *N Engl J Med*. 2012;367(11):991-1001. doi: 10.1056/NEJMoa1205361.
5. Tesche C, De Cecco CN, Baumann S, Renker M, McLaurin TW, Duguay TM, et al. Coronary CT Angiography-derived Fractional Flow Reserve: Machine Learning Algorithm versus Computational Fluid Dynamics Modeling. *Radiology*. 2018;288(1):64-72. doi: 10.1148/radiol.2018171291.
6. Cury RC, Magalhães TA, Borges AC, Shiozaki AA, Lemos PA, Soares J Jr, et al. Dipyridamole Stress and Rest Myocardial Perfusion by 64-detector Row Computed Tomography in Patients with Suspected Coronary Artery Disease. *Am J Cardiol*. 2010;106(3):310-5. doi: 10.1016/j.amjcard.2010.03.025.
7. Tomizawa N, Chou S, Fujino Y, Kamitani M, Yamamoto K, Inoh S, et al. Feasibility of Dynamic Myocardial CT Perfusion Using Single-source 64-row CT. *J Cardiovasc Comput Tomogr*. 2019;13(1):55-61. doi: 10.1016/j.jcct.2018.10.003.
8. Danad I, Szymonifka J, Schulman-Marcus J, Min JK. Static and Dynamic Assessment of Myocardial Perfusion by Computed Tomography. *Eur Heart J Cardiovasc Imaging*. 2016;17(8):836-44. doi: 10.1093/ehjci/jew044.
9. Mushtaq S, Conte E, Pontone G, Baggiano A, Annoni A, Formenti A, et al. State-of-the-art-myocardial Perfusion Stress Testing: Static CT Perfusion. *J Cardiovasc Comput Tomogr*. 2020;14(4):294-302. doi: 10.1016/j.jcct.2019.09.002.
10. Magalhães TA, Cury RC, Cerci RJ, Parga JR Filho, Gottlieb I, Nacif MS, et al. Evaluation of Myocardial Perfusion by Computed Tomography - Principles, Technical Background and Recommendations. *Arq Bras Cardiol*. 2019;113(4):758-67. doi: 10.5935/abc.20190217.
11. Mehra VC, Valdiviezo C, Arbab-Zadeh A, Ko BS, Seneviratne SK, Cerci R, et al. A Stepwise Approach to the Visual Interpretation of CT-based Myocardial Perfusion. *J Cardiovasc Comput Tomogr*. 2011;5(6):357-69. doi: 10.1016/j.jcct.2011.10.010.
12. Taylor CA, Fonte TA, Min JK. Computational Fluid Dynamics Applied to Cardiac Computed Tomography for Noninvasive Quantification of Fractional Flow Reserve: Scientific Basis. *J Am Coll Cardiol*. 2013;61(22):2233-41. doi: 10.1016/j.jacc.2012.11.083.
13. Koo BK, Erglis A, Doh JH, Daniels DV, Jegere S, Kim HS, et al. Diagnosis of Ischemia-causing Coronary Stenoses by Noninvasive Fractional Flow Reserve Computed from Coronary Computed Tomographic Angiograms. Results from the Prospective Multicenter DISCOVER-FLOW (Diagnosis of Ischemia-Causing Stenoses Obtained Via Noninvasive Fractional Flow Reserve) Study. *J Am Coll Cardiol*. 2011;58(19):1989-97. doi: 10.1016/j.jacc.2011.06.066.
14. Min JK, Leipsic J, Pencina MJ, Berman DS, Koo BK, van Mieghem C, et al. Diagnostic Accuracy of Fractional Flow Reserve from Anatomic CT Angiography. *JAMA*. 2012;308(12):1237-45. doi: 10.1001/2012.jama.11274.
15. Leipsic J, Yang TH, Thompson A, Koo BK, Mancini GB, Taylor C, et al. CT Angiography (CTA) and Diagnostic Performance of Noninvasive Fractional Flow Reserve: Results from the Determination of Fractional Flow Reserve by Anatomic CTA (DeFACTO) Study. *AJR Am J Roentgenol*. 2014;202(5):989-94. doi: 10.2214/AJR.13.11441.
16. Nørgaard BL, Leipsic J, Gaur S, Seneviratne S, Ko BS, Ito H, et al. Diagnostic Performance of Noninvasive Fractional Flow Reserve Derived from Coronary Computed Tomography Angiography in Suspected Coronary Artery Disease: The NXT Trial (Analysis of Coronary Blood Flow Using CT Angiography: Next Steps). *J Am Coll Cardiol*. 2014;63(12):1145-55. doi: 10.1016/j.jacc.2013.11.043.
17. Douglas PS, Pontone G, Hlatky MA, Patel MR, Nørgaard BL, Byrne RA, et al. Clinical Outcomes of Fractional Flow Reserve by Computed Tomographic Angiography-guided Diagnostic Strategies vs. Usual Care in Patients with Suspected Coronary Artery Disease: The Prospective Longitudinal Trial of FFR(CT): Outcome and Resource Impacts Study. *Eur Heart J*. 2015;36(47):3359-67. doi: 10.1093/eurheartj/ehv444.
18. Patel MR, Nørgaard BL, Fairbairn TA, Nieman K, Akasaka T, Berman DS, et al. 1-Year Impact on Medical Practice and Clinical Outcomes of FFRCT: The ADVANCE Registry. *JACC Cardiovasc Imaging*. 2020;13(1 Pt 1):97-105. doi: 10.1016/j.jcmg.2019.03.003.
19. Itu L, Rapaka S, Passerini T, Georgescu B, Schwemmer C, Schoebinger M, et al. A Machine-learning Approach for Computation of Fractional Flow Reserve from Coronary Computed Tomography. *J Appl Physiol*. 2016;121(1):42-52. doi: 10.1152/jappphysiol.00752.2015.
20. Fujimoto S, Kawasaki T, Kumamaru KK, Kawaguchi Y, Dohi T, Okonogi T, et al. Diagnostic Performance of On-site Computed CT-fractional Flow Reserve Based on Fluid Structure Interactions: Comparison with Invasive Fractional Flow Reserve and Instantaneous Wave-free ratio. *Eur Heart J Cardiovasc Imaging*. 2019;20(3):343-52. doi: 10.1093/ehjci/jev104.
21. Abbara S, Arbab-Zadeh A, Callister TQ, Desai MY, Mamuya W, Thomson L, et al. SCCT Guidelines for Performance of Coronary Computed Tomographic Angiography: A Report of the Society of Cardiovascular Computed Tomography Guidelines Committee. *J Cardiovasc Comput Tomogr*. 2009;3(3):190-204. doi: 10.1016/j.jcct.2009.03.004.
22. Nørgaard BL, Gaur S, Leipsic J, Ito H, Miyoshi T, Park SJ, et al. Influence of Coronary Calcification on the Diagnostic Performance of CT Angiography Derived FFR in Coronary Artery Disease: A Substudy of the NXT Trial. *JACC Cardiovasc Imaging*. 2015;8(9):1045-55. doi: 10.1016/j.jcmg.2015.06.003.



This is an open-access article distributed under the terms of the Creative Commons Attribution License